Korean J. Chem. Eng., 32(1), 141-148 (2015)
DOI: 10.1007/s11814-014-0193-1

pISSN: 0256-1115
eISSN: 1975-7220

Density measurement and equal density temperature of CO_2+brine from Dagang - formation from 313 to 363 K

Yi Zhang, Weiwei Jian†, Yangchun Zhan, Yongchen Song, Mingjun Yang, Jiafei Zhao, Yu Liu, Weiguo Liu, and Yong Shen

Key Laboratory of Ocean Energy Utilization and Energy Conservation of Ministry of Education, School of Energy and Power Engineering, Dalian University of Technology, Dalian, Liaoning 116024, P. R. China
(*Received 25 January 2014 • accepted 9 July 2014*)

Abstract−Densities of CO_2+Dagang - formation brine solution were measured by a magnetic suspension balance (MSB) in the pressure range from (10 to 18) MPa, at the temperatures from (313.15 to 363.15) K and CO_2 mass fractions at 0, 0.0101, 0.0198 and 0.0299. The experimental results revealed that the solution densities increased linearly with the increasing pressure and CO_2 concentration, while decreasing with the increasing temperatures in the experimental range. When the temperature increased from (313.15 to 363.15) K, the slopes of the densities versus (*vs.*) CO_2 mass fractions decreased from (0.193 to 0.106) g·cm^{-3}. A correlation equation was developed based on thermodynamic theory and experimental data. The absolute average deviation between the correlation equation and the experimental data was 0.05%, and the maximum deviation was 0.37% for the density of CO_2+water/brine solution in common geological storage conditions. According to the density of CO_2 - free brine and apparent molar volume of CO_2 in brine, the equal density temperature (T_e) of CO_2+Dagang brine solution was obtained at 464.67 K when pressure is 10 MPa, which means that the density of brine dissolved with CO_2 will be less than that of CO_2-free brine when the temperature is higher than 464.67 K at 10 MPa. In this work the formation temperature of the Dagang oilfield reservoir is from 313.15 K to 363.15 K, which is lower than the equal density temperature. Therefore, the safety of CO_2 storage in Dagang oilfield reservoir can be guaranteed.

Keywords: Density, CO_2, Brine, Equal Density Temperature, Magnetic Suspension Balance

INTRODUCTION

Burning of fossil fuels produces a large amount of carbon dioxide, which has led to serious irreversible changes to the global climate [1]. A very promising approach to reducing CO_2 emissions is its capture at a certain site, transport to an injection site and sequestration in suitable geologic formations [2-5]. The saline aquifer presents the largest capacity available for CO_2 storage among all geological options [6]. CO_2+water and CO_2+brine are fundamental and typical fluids in geological stratification [7]. Density and viscosity of liquids are important physicochemical properties which affect mass and heat transfer in solutions [8]. The density of CO_2 aqueous solution has an important impact on the safety of CO_2 sequestration. Especially, predicting the migration of CO_2 in geological storage needs high precision density data [9]. The density change is very small when CO_2 dissolves in aqueous solution, while a density difference of 0.1 g·cm^{-3} is sufficient to drive a natural CO_2 solution to either sink or buoy [10]. Therefore, the density of CO_2+water/brine solution as a function of temperature, pressure and salinity is an important physicochemical property for CCS.

The density of CO_2+water/brine solution has been largely studied in the past twenty years. Ohsumi et al. [11] measured the densities of liquid CO_2 solution at low CO_2 concentrations at 276.15 K and 34.754 MPa by applying a vibrating - type densitometer. Song et al. [12] measured the densities of CO_2+seawater solution at 276.15 K and 283.15 K and pressure range from (4.0 to 12.0) MPa using Mach - Zehnder interferometry. The experimental results revealed that the density difference between CO_2+seawater and pure seawater is linearly proportional to the CO_2 mass fraction and independent on pressure, temperature, and salinity. Densities of deionized water and Weyburn - Formation brine were obtained for both the saturated and unsaturated CO_2 solution in the aqueous phase by Li et al. [13] at 332.15 K and pressures up to 29 MPa. The measured density of aqueous CO_2 solution was correlated as a function of CO_2 concentration and pressure. Zhang et al. [14] obtained the densities of CO_2+ Tianjin - Tanggu brine solution using a magnetic suspension balance at pressure from (10 to 18) MPa, temperature from (313 to 353) K and CO_2 mass fractions up to 0.040. Two regression functions were developed to describe the density data of CO_2 - free and CO_2+brine solution, and the prediction errors were within 0.004% and 0.03%.

In addition, Song et al. [15] reported the densities for CO_2+H_2O system from 274.15 to 413.15 K, pressures up to 18 MPa and CO_2 mole fraction of x_1=(0, 0.0042, 0.0084, and 0.0124). The partial molar volumes were calculated by the experimental densities and PC-SAFT and tPC-PSAFT models were used to predict the CO_2 aqueous solution. Yan et al. [16] reported the densities of CO_2 in 0, 1 and 5 mol/kg NaCl brine at 323 K, 373 K and 413 K and pres-

†To whom correspondence should be addressed.
E-mail: happywei1988@126.com

sure range from (5 to 40) MPa. It is shown that the dissolution of CO_2 increases the brine density only if the apparent mass density of CO_2 in brine is higher that the brine density at the same conditions. According to the analysis of Hu et al. [17], most of these density data were not in agreement with each other and the accuracy cannot satisfy the requirement of CO_2 geological sequestration.

In common conditions, the brine density will increase with the dissolution of CO_2, which will cause the CO_2+brine solution to sink to the bottom of the formation and enhance the safety of CCS. While, Lu et al. [18] showed that the density of CO_2+brine solution may be lower than that of CO_2 - free brine when the temperature is higher than 393 K for high salinity solution. The result is simulated by different equations of states but lack of adequate experimental data. Therefore, more density experiments should be performed for CO_2+brine solution under practical sequestration conditions.

It is understood that the dissolution of CO_2 in aqueous solution depends on pressure, temperature and the salt concentration, which are not universally constant for different reservoirs. To develop an analytical expression for estimating density for CO_2 sequestration, reliable density data under different experimental conditions are necessary. Supported by the National High Technology Research and Development Program of China, 300 tons of CO_2 have been sequestered in Dagang Oilfield, located at the southeast of Tianjin city of China in 2012. The purpose of this pilot project is CO_2 sequestration and enhanced oil recovery in residual oilfield by G6 - 35 well. Therefore, brine from Dagang - oilfield reservoir was selected as the sample brine. To provide high precision density data and model for practical geological storage project, this paper reports the experimental densities of CO_2+brine from Dagang - oilfield reservoir.

EXPERIMENTAL SECTION

According to the practical pressure and temperature range of Dagang - oilfield reservoir, density experiments were performed at pressures from (10 to 18) MPa and temperatures from (313.15 to 363.15) K. It is generally believed that the solubility of CO_2 in water/brine increases with the increasing pressure and decreases with the temperature. CO_2 solubility in pure water is 0.035 at 363.15 K and 10.00 MPa provided by National Institute of Standards and Technology. Li et al. [13] reported the CO_2 mass fraction in Weyburn brine was 0.0339 at 332.15 K and 10.38 MPa. And Yan et al. [16] measured that the CO_2 solubility was 0.0292 at 373.2 K, 10.00 MPa in 1 mol/kg NaCl brine. To ensure that the CO_2 would dissolve in the brine completely during the measurement, the CO_2 mass fraction in Dagang - Formation brine was selected up to 0.0300.

1. Experimental Apparatus

Fig. 1 is a schematic diagram of the experimental apparatus and Fig. 2 shows the detail of the magnetic suspension balance. The MSB consists of a microbalance, a permanent magnet, an electromagnet, a sensor core, a sinker and a device for coupling/decoupling the measuring load (Fig. 2). The measuring force is transferred contactlessly from the measuring cell to the microbalance by the interaction between electromagnet and permanent magnet. The microbalance is isolated from the measuring sample so that the

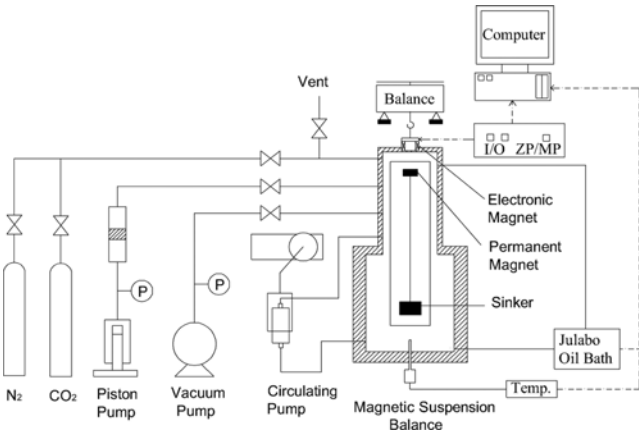

Fig. 1. Schematic diagram of the experimental apparatus.

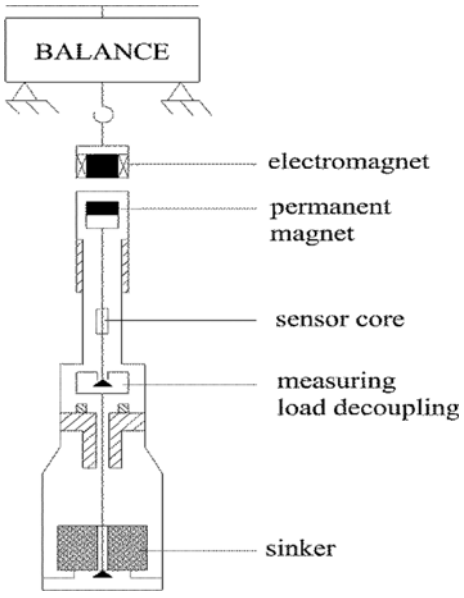

Fig. 2. Details of the magnetic suspension balance.

MSB can be used in high temperature, high pressure, vacuum or corrosive environment. The MSB can be tared and calibrated automatically at zero point by the measuring load decoupling device in the measurement so high precision can be obtained.

The measuring range of the MSB in our laboratory was that pressure from vacuum to 20 MPa and temperature from (253 to 423) K. The temperature and pressure in the measuring cell were obtained with a Pt100 temperature probe (resolution internal 0.01 K) and a pressure sensor (20 MPa, reproducibility 0.08%), respectively. For a detailed description of the system control and operation refer to Zhang et al. [14].

2. Experimental Material

The experimental gases such as CO_2 and N_2 were provided by Dalian Da-te Gas Co., Ltd. The mole fraction purity of CO_2 and N_2 was 0.9999 and 0.99999, respectively. The analysis methods were gas chromatography and dew point method. All the chemicals were used without any further purification. The experimental brine was collected at the wellhead of the G6 - 35 well in Dagang - oilfield,

Table 1. The Composition of brine sample from Dagang - formation

Ions	Concentration ($mg \cdot L^{-1}$)	Analysis method	Apparatus
Sodium	1513.60	Atomic absorption spectrometry	Solar, Unicam 969
Potassium	11.64	Atomic absorption spectrometry	Solar, Unicam 969
Calcium	9.86	Atomic absorption spectrometry	Solar, Unicam 969
Magnesium	3.21	Atomic absorption spectrometry	Solar, Unicam 969
Iron	0.03	Atomic absorption spectrometry	Solar, Unicam 969
Fluoride	2.72	Ion chromatography	Dionex ICS-90
Chloride	1294.00	Ion chromatography	Dionex ICS-90
Sulfate	0.43	Ion chromatography	Dionex ICS-90
Bicarbonate	1815.95	Valence conservation	None

and the brine sample belonged to the bottomhole sample at a depth of (1640 to 1829) meter underneath the land surface. The cations of the brine sample were analyzed using a Solar 969 Unicam series atomic absorption spectrophotometer (AAS), and the anions were determined by the Dionex ICS-90 ion chromatograph with AMMS III4mm suppressor and DS5 conductivity detector. The leachate was 9 $mmol \cdot L^{-1}$ Na_2CO_3, the regeneration fluid was 50 $mmol \cdot L^{-1}$ H_2SO_4 and the flow velocity was 1.0 $mL \cdot min^{-1}$. The composition of the brine sample is presented in Table 1. The salinity of Dagang brine was converted to NaCl concentration as 0.08027 mol/kg.

3. Experimental Procedure

Before the experiment, air tightness detection was performed on the experimental system, and the measuring cell was evacuated with a vacuum pump. Then CO_2 and brine were injected into the measuring cell successively. The CO_2+brine solution was homogenized by a circulating pump (AKICO, Japan), which could also accelerate the dissolution of CO_2. The pressure and temperature of the solution were regulated by a piston pump and a circulating liquid thermostat (controlling accuracy ±0.01 K) respectively. The mass fraction of CO_2 in solution was determined by the ratio between the CO_2 density and the solution density because the volume change of the measuring cell due to the injection of brine can be neglected. If the temperature, pressure and MSB readout achieved a stable state, the uniform state of CO_2+brine mixture was reached and the density of CO_2+brine solution could be recorded.

4. Experimental Principle

The basic principle of density measurement by MSB is the Archimedean principle. The sinker immersed in the brine solution undergoes an apparent loss in weight, which is equal to the weight of the brine solution it displaces. Therefore, the density of the sample solution can be calculated from

$$\rho_{(T,P)} = \frac{m_0 - m'_{(T,P)}}{v_{(T,P)}} \tag{1}$$

where $\rho_{(T,P)}$ is the solution density under measuring conditions (T, P). m_0 is the mass value of sinker in vacuum. $m'_{(T,P)}$ is the apparent mass value of sinker under measuring conditions (T, P). $v_{(T,P)}$ is the volume of sinker under measuring conditions (T, P).

The uncertainty of the solution densities can be calculated by Eq. (2).

$$U(\rho) = \{[U_d(\rho)]^2 + [U(w)]^2\}^{1/2} \tag{2}$$

$$U_d(\rho) = \sqrt{\left(\frac{\partial \rho}{\partial m_0}\right)^2 U_{m_0}^2 + \left(\frac{\partial \rho}{\partial m'}\right)^2 U_{m'}^2 + \left(\frac{\partial \rho}{\partial v}\right)^2 U_v^2} \tag{3}$$

where $U(\rho)$, $U_d(\rho)$, U(w) is the uncertainty of solution density, measured density and mass fraction, U_{m_0}, U_m and U_v represent the uncertainty of measured density caused by m_0, m' and v respectively.

The influence of temperature on the density is mainly manifested in the volume change of the sinker. The value of $v_{(T,P)}$ can be calculated by Eq. (4) [14].

$$v_{(T,P)} = v_{(T_0,P_0)}\left[1 + \alpha_T(T - T_0) - \frac{1}{K_T}(P - P_0)\right] \tag{4}$$

where $v_{(T_0,P_0)}$ is the sinker volume at reference state (T_0, P_0), α_T is the isobaric thermal expansion coefficient and K_T is the isothermal compressibility module. These parameters can be calculated from the following equations:

$$\alpha_T = \frac{\Delta L}{L_0} \cdot \frac{1}{(T - T_0)} \tag{5}$$

$$K_T = \frac{E}{3 - 6\gamma} \tag{6}$$

$$E = -3\times10^{-13}T^6 + 3\times10^{-10}T^5 - 9\times10^{-8}T^4 + 1\times10^{-5}T^3 - 1\times10^{-3}T^2 + 0.194T + 92.71 \tag{7}$$

$$\gamma = -6\times10^{-14}T^5 + 3\times10^{-11}T^4 - 5\times10^{-9}T^3 + 1\times10^{-7}T^2 - 1\times10^{-4}T + 0.339 \tag{8}$$

where L_0 is original length of the sinker, ΔL is the length change of the sinker, E is Young's modulus and γ is Poisson's ratio.

Standard uncertainty is U (T)=0.01 K, U (P)=0.001 MPa, U (w)= 0.0001 and the combined expanded uncertainties of solution densities are U (ρ)=2•0.13 $kg \cdot m^{-3}$ (0.95 level of confidence).

RESULTS AND DISCUSSION

The densities of CO_2+Dagang brine solution were measured in the pressure range from (10 to 18) MPa, at the temperatures from (313.15 to 363.15) K. The measured densities are presented in Tables 2 to 5 for CO_2 mass fractions at 0, 0.0101, 0.0198 and 0.0299.

1. Experimental Densities

Experimental densities are presented graphically as a function of pressure at different temperatures and CO_2 mass fractions in Fig. 3.

Table 2. Experimental densities (ρ)[a] of CO_2+brine from Dagang - formation (w=0)[b]

T/K	P/MPa	ρ/g·cm^{-3}	T/K	P/MPa	ρ/g·cm^{-3}
313.11	9.994	0.99933	343.26	9.995	0.98480
313.11	10.997	0.99966	343.26	10.993	0.98514
313.09	12.006	1.00000	343.27	12.002	0.98548
313.09	13.006	1.00034	343.28	12.992	0.98582
313.09	14.010	1.00068	343.29	13.987	0.98615
313.10	14.997	1.00100	343.31	14.993	0.98647
313.11	16.003	1.00134	343.32	16.002	0.98682
313.12	17.005	1.00167	343.29	17.003	0.98716
313.15	18.010	1.00199	343.31	18.010	0.98750
323.15	10.001	0.99508	353.13	9.988	0.97896
323.16	10.998	0.99541	353.09	11.007	0.97934
323.14	12.008	0.99576	353.13	12.014	0.97967
323.11	13.007	0.99610	353.13	13.003	0.98001
323.10	14.000	0.99644	353.11	14.009	0.98037
323.11	15.007	0.99677	353.12	15.005	0.98071
323.13	15.999	0.99710	353.11	16.003	0.98107
323.09	17.001	0.99745	353.13	17.005	0.98141
323.12	18.001	0.99776	353.13	18.005	0.98175
333.18	9.998	0.99024	363.27	10.001	0.97247
333.16	11.002	0.99058	363.28	10.998	0.97283
333.16	12.001	0.99091	363.28	12.004	0.97320
333.17	13.000	0.99124	363.27	12.998	0.97355
333.18	13.993	0.99157	363.27	14.003	0.97391
333.18	15.001	0.99191	363.27	14.999	0.97428
333.18	15.998	0.99225	363.27	16.000	0.97463
333.18	16.990	0.99258	363.27	17.001	0.97498
333.19	18.004	0.99291	363.28	18.001	0.97534

[a]Standard uncertainty u are U (T)=0.01 K, U (P)=0.001 MPa, U (w)= 0.0001 and the combined expanded uncertainties of measured densities are U (ρ)=2•0.13 kg·m^{-3} (0.95 level of confidence)
[b]w represents the mass fraction of CO_2 in brine is 0

Table 3. Experimental densities (ρ)[a] of CO_2+brine from Dagang - formation (w=0.0101)[b]

T/K	P/MPa	ρ/g·cm^{-3}	T/K	P/MPa	ρ/g·cm^{-3}
313.17	10.003	1.00116	343.13	9.998	0.98644
313.19	10.998	1.00149	343.12	10.998	0.98679
313.20	12.009	1.00182	343.10	11.997	0.98715
313.22	12.998	1.00215	343.14	13.003	0.98744
313.24	14.003	1.00248	343.12	13.998	0.98777
313.25	15.000	1.00282	343.11	14.998	0.98811
313.24	16.008	1.00316	343.15	15.999	0.98841
313.22	17.000	1.00350	343.17	17.001	0.98874
313.21	18.003	1.00385	343.18	17.997	0.98907
323.13	9.993	0.99702	353.19	10.003	0.98039
323.12	11.002	0.99737	353.16	11.000	0.98076
323.13	12.000	0.99771	353.13	12.006	0.98114
323.12	12.992	0.99804	353.11	13.010	0.98155
323.12	13.998	0.99837	353.11	13.996	0.98195
323.11	14.994	0.99870	353.09	15.006	0.98230
323.14	16.007	0.99901	353.12	16.006	0.98262
323.20	16.992	0.99929	353.15	16.999	0.98293
323.20	18.002	0.99963	353.17	18.005	0.98326
333.09	10.002	0.99211	363.23	9.994	0.97348
333.10	11.011	0.99244	363.22	11.001	0.97386
333.10	11.999	0.99277	363.22	12.008	0.97423
333.11	13.001	0.99311	363.25	13.001	0.97456
333.11	13.995	0.99344	363.26	13.997	0.97491
333.10	15.003	0.99379	363.28	14.993	0.97525
333.09	16.003	0.99413	363.25	16.003	0.97563
333.08	17.004	0.99447	363.27	17.005	0.97602
333.09	18.007	0.99479	363.24	17.998	0.97644

[a]Standard uncertainty u are U (T)=0.01 K, U (P)=0.001 MPa, U (w)= 0.0001 and the combined expanded uncertainties of measured densities are U (ρ)=2•0.13 kg·m^{-3} (0.95 level of confidence)
[b]w represents the mass fraction of CO_2 in brine is 0.0101

The densities of CO_2+Dagang - formation brine increase almost linearly with pressure at constant temperatures and CO_2 concentrations. And the slopes of the fitting curves of densities *vs.* pressures are almost the same for different CO_2 concentrations at the same temperature. All isotherms in Fig. 3 show that the brine densities dissolved with CO_2 are larger than those of CO_2 - free brine in our experimental range. The possible explanation may be that the partial density of dissolved CO_2 is larger than brine density for a typical temperature condition [19]. As shown in Fig. 3, with the increasing temperature the solution densities decrease and the density differences between solutions with different CO_2 concentrations become smaller.

Fig. 4 exhibits the densities of CO_2+Dagang - formation brine solution *vs.* CO_2 mass fraction at 14 MPa. As one can see, the densities of CO_2+Dagang - formation brine increase with increasing CO_2 mass fractions almost linearly at constant pressures and temperatures, which is consistent with previous studies [9,14,20]. But the slopes of the fitting curves of solution densities *vs.* CO_2 mass fractions decrease from (0.193 to 0.106) g·cm^{-3} with the temperature increase from (313.15 to 363.15) K.

2. Correlation Equation

The salinity of Dagang brine was converted to NaCl concentration as 0.08027 mol/kg according to the concentration of various ion components in Table 1. The density of CO_2-free Dagang brine can be predicted by the model of Rogers and Pitzer [20] which has good extrapolations. The maximum deviation and the average deviation is 0.11% and 0.08%, respectively.

If the brine is regarded as a pure substance for CO_2+brine solution system, the volume of pseudo binary solution can be expressed as

$$V_m = x_1 V_1 + x_2 V_2^{\phi} \quad (9)$$

where V_m is the molar volume of the CO_2+brine solution, x_1 and x_2 are the mole fractions of brine and CO_2, respectively; V_1 is the molar volume of brine and V_2^{ϕ} is the apparent molar volume of CO_2 dissolved in brine.

Assuming that 1 g brine solution containing dissolved CO_2, we

Table 4. Experimental densities (ρ)[a] of CO_2+brine from Dagang - formation (w=0.0198)[b]

T/K	P/MPa	ρ/g·cm^{-3}	T/K	P/MPa	ρ/g·cm^{-3}
313.07	10.007	1.00303	343.28	9.995	0.98811
313.10	10.998	1.00335	343.28	11.004	0.98846
313.11	11.996	1.00368	343.28	12.002	0.98880
313.10	12.998	1.00403	343.29	12.995	0.98913
313.08	14.002	1.00436	343.29	13.999	0.98947
313.06	14.998	1.00471	343.28	14.996	0.98982
313.09	15.999	1.00504	343.26	15.994	0.99016
313.07	16.998	1.00538	343.27	16.995	0.99050
313.09	18.003	1.00571	343.27	18.010	0.99084
323.27	10.000	0.99891	353.13	9.992	0.98195
323.29	11.000	0.99924	353.12	11.009	0.98232
323.29	11.998	0.99957	353.07	12.007	0.98269
323.26	12.999	0.99992	353.07	13.009	0.98304
323.21	14.003	1.00028	353.08	14.004	0.98338
323.22	14.998	1.00060	353.07	15.001	0.98374
323.24	16.013	1.00093	353.08	16.002	0.98406
323.26	17.003	1.00125	353.18	16.996	0.98433
323.30	18.004	1.00156	353.20	17.999	0.98466
333.10	9.999	0.99393	363.26	9.995	0.97469
333.10	10.996	0.99427	363.25	10.997	0.97504
333.09	12.001	0.99462	363.25	11.997	0.97540
333.05	12.994	0.99498	363.25	13.001	0.97576
333.11	14.000	0.99530	363.28	13.996	0.97610
333.10	14.999	0.99562	363.27	14.995	0.97645
333.10	15.998	0.99596	363.26	16.003	0.97683
333.08	16.995	0.99631	363.25	17.005	0.97720
333.04	17.999	0.99666	363.25	18.011	0.97756

[a]Standard uncertainty u are U (T)=0.01 K, U (P)=0.001 MPa, U (w)= 0.0001 and the combined expanded uncertainties of measured densities are U (ρ)=2•0.13 kg·m^{-3} (0.95 level of confidence)
[b]w represent the mass fraction of CO_2 in brine is 0.0198

Table 5. Experimental densities (ρ)[a] of CO_2+brine from Dagang - formation (w=0.0299)[b]

T/K	P/MPa	ρ/g·cm^{-3}	T/K	P/MPa	ρ/g·cm^{-3}
313.11	9.997	1.00510	343.15	10.004	0.98972
313.13	11.000	1.00543	343.14	11.004	0.99008
313.12	11.996	1.00577	343.15	11.999	0.99042
313.08	12.997	1.00612	343.15	13.003	0.99076
313.08	14.004	1.00645	343.15	13.998	0.99110
313.09	15.000	1.00677	343.17	14.995	0.99144
313.12	16.007	1.00710	343.18	15.992	0.99178
313.10	16.997	1.00744	343.18	17.003	0.99213
313.09	17.996	1.00778	343.17	18.000	0.99247
323.08	10.003	1.00084	353.18	10.003	0.98321
323.07	11.000	1.00118	353.16	11.000	0.98358
323.09	11.997	1.00151	353.15	11.996	0.98394
323.09	12.999	1.00185	353.11	12.999	0.98432
323.08	14.005	1.00218	353.13	13.994	0.98464
323.08	15.001	1.00251	353.14	15.000	0.98500
323.08	15.999	1.00284	353.18	16.002	0.98533
323.07	16.900	1.00310	353.16	17.003	0.98569
323.07	18.002	1.00351	353.17	18.008	0.98603
333.22	10.002	0.99576	363.22	9.996	0.97564
333.24	10.999	0.99607	363.25	11.001	0.97593
333.25	11.998	0.99642	363.22	12.003	0.97631
333.24	12.998	0.99676	363.23	12.995	0.97669
333.23	14.004	0.99710	363.27	13.998	0.97702
333.22	15.000	0.99745	363.26	14.999	0.97737
333.25	16.003	0.99777	363.24	16.008	0.97776
333.24	17.003	0.99811	363.24	17.005	0.97813
333.24	18.009	0.99844	363.27	17.997	0.97846

[a]Standard uncertainty u are U (T)=0.01 K, U (P)=0.001 MPa, U (w)= 0.0001 and the combined expanded uncertainties of measured densities are U (ρ)=2•0.13 kg·m^{-3} (0.95 level of confidence)
[b]w represents the mass fraction of CO_2 in brine is 0.0299

can obtain:

$$\frac{1}{M}V_m=\frac{1-w_2}{M_1}V_1+\frac{w_2}{M_2}V_2^{\phi} \tag{10}$$

where M, M_1 and M_2 are the relative molecular weight of the pseudo binary solution, brine and CO_2, respectively. is the mass fraction of CO_2.

Introducing mass density allows the Eq. (10) to be simple:

$$\frac{1}{\rho^m}=\frac{1-w_2}{\rho_1^m}+\frac{w_2}{\rho_2^{m,\phi}} \tag{11}$$

where ρ^m and ρ_1^m are the mass density of the solution and brine, respectively; $\rho_2^{m,\phi}$ is the apparent mass density of CO_2 which can be obtained by Eq. (12).

$$\rho_2^{m,\phi}=\frac{M_2}{V_2^{\phi}}=\frac{44.01}{V_2^{\phi}} \tag{12}$$

The apparent molar volume of CO_2 in water V_2^{ϕ} was represented as a function of temperature in Garcia et al. [21], while the effect of pressure and brine salinity on the apparent molar volume cannot be neglected for CO_2+brine solution. So based on our experimental data and previous literature data such as Song et al. [12], Li et al. [13], Yan et al. [16], and Hnedkovsky et al. [22], the apparent molar volume of CO_2 can be expressed as a function of temperature, pressure and salinity of the brine:

$$V_2^{\varphi}=\sum_{i=0}^{3}a_iT^i+\sum_{i=1}^{2}b_i\frac{p}{T^i}+\sum_{i=1}^{3}c_ip^i+\sum_{i=1}^{3}d_is^i \tag{13}$$

where T (K) is temperature, p (MPa) is the pressure, s (mol·kg^{-1}) is the salinity of brine, a_i, b_i, c_i and d_i are the coefficients of Eq. (13) which are listed in Table 6. This model is compared with the extensive experimental data as shown in Fig. 5. As one can see, the prediction results are well in agreement with the experimental data in the temperature range from 273.25 to 523.15 K and pressures from 0.7 to 40 MPa.

Through proper simplification of Eq. (11), the CO_2 solution density can be obtained from Eq. (14):

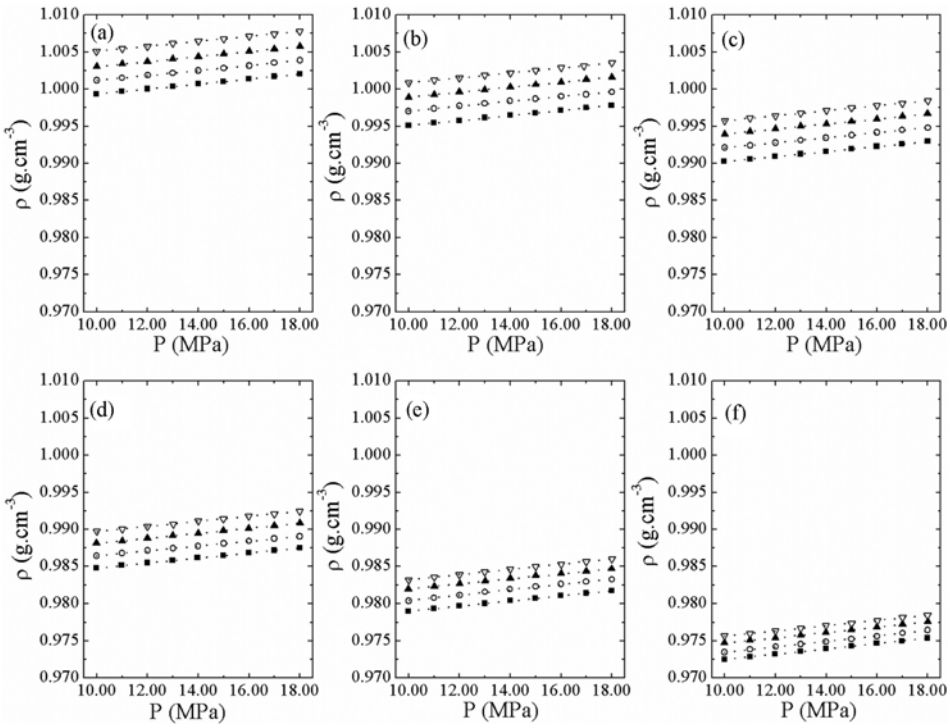

Fig. 3. Densities of CO_2+brine solution from Dagang - formation versus pressure P/MPa at different temperatures and CO_2 concentrations: (a) 313 K; (b) 323 K; (c) 333 K; (d) 343 K; (e) 353 K; (f) 363 K; ■, w=0; ○, w=0.0101; ▲, w=0.0198; ▽, w=0.0299.

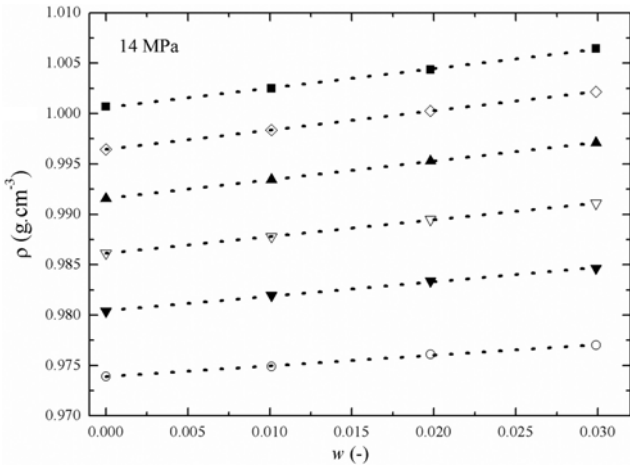

Fig. 4. Densities of CO_2+brine solution from Dagang - formation versus CO_2 mass fractions at 14 MPa under different temperature: ■, 313 K; ◇, 323 K; ▲, 333 K; ▽, 343 K; ▼, 353 K; ○, 363 K.

$$\rho^m = \frac{44.01\rho_1^m}{44.01(1-w_2)+\rho_1^m w_2 V_2^\phi} \quad (14)$$

The correlation equation is compared with the experimental density of previous literature data from Li et al. [13] Yan et al. [16], Hnedkovsky et al. [22], Song et al. [23], King et al. [24] and Hebach et al. [25]. It is notable that the experimental data of Li et al. [13] has systematic deviations which can be corrected according to Hu et al. [17]. The comparison results are shown in Fig. 6. The absolute average deviation between the correlation equation and the

Table 6. Coefficients in Eq. (13)

i	a_i	b_i	c_i	d_i
0	−59.88537	/	/	/
1	0.7288477	−19.35352	−0.342608	15.22761
2	-0.1946607×10^{-2}	11513.26	0.01350698	−18.4242
3	0.1916996×10^{-5}	/	0.185219×10^{-3}	3.01823

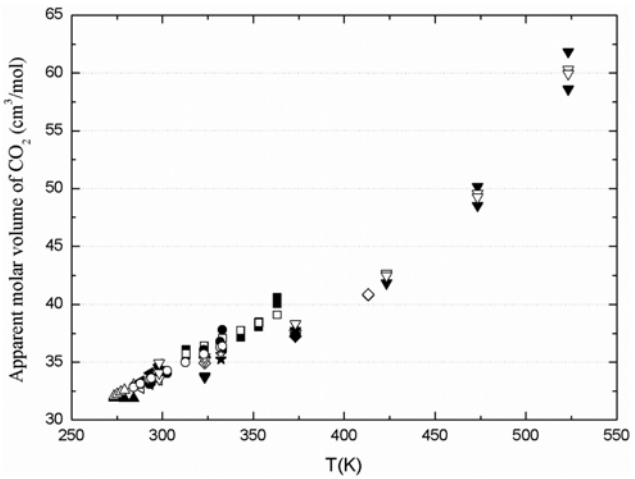

Fig. 5. Apparent molar volume of dissolved CO_2 of this work and literatures: □, ■ This work: ☆, ★ Li et al. [13]; ◇, ◆ Yan et al. [16]; ▽, ▼ Hnedkovsky et al. [22];△, ▲ Song et al. [23]; ◁, ◀ King et al. [24]; ○, ● Hebach et al. [25]. The solid symbols are experimental results and the open symbols are results predicted by Eq. (13).

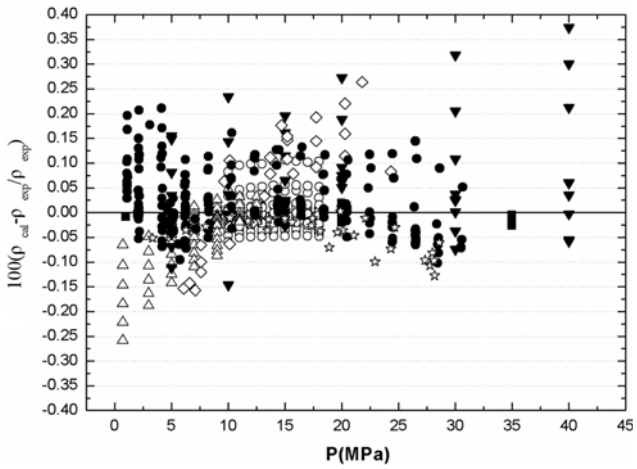

Fig. 6. Deviations of experimental densities ρ_{exp} and ρ_{cal} from the correlation of Eq. (14) versus pressure P/MPa: ○, This work: ☆, Li et al. [13]; ▼, Yan et al. [16]; ■, Hnedkovsky et al. [22]; △, Song et al. [23]; ◇, King et al. [24]; ●, Hebach et al. [25].

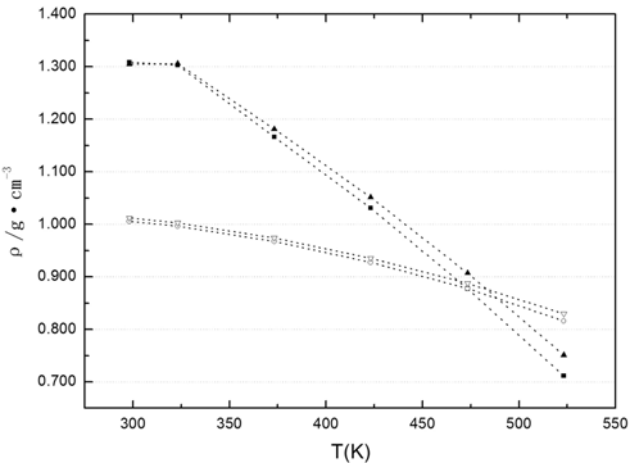

Fig. 8. Experimental density of pure water in Hnedkovsky et al. [22] (○, 20 MPa; ▽, 35 MPa) and apparent mass density of dissolved CO_2 (■, 20 MPa; ▲, 35 MPa) as a function of temperature.

experimental data was 0.05% and the maximum deviation was 0.37%. Therefore, the correlation equation can accurately represent the experimental density of CO_2+water and CO_2+brine solution in a wide temperature ranges from 273.25 K to 523.15 K.

3. Equal Density Temperature

Eq. (15) can be obtained by rearranging Eq. (11).

$$\rho^m = \left[1 + w_2\left(\frac{\rho_1^m}{\rho_2^{m,\phi}} - 1\right)\right]^{-1} \rho_1^m \tag{15}$$

Obviously, if ρ_1^m is larger than $\rho_2^{m,\phi}$, ρ^m will be smaller than ρ_1^m, which means that the brine density will decrease after CO_2 dissolution. Figs. 7 and 8 display ρ_1^m and $\rho_2^{m,\phi}$ at different pressures and salinities. The density of CO_2 - free brine is predicted with model of Rogers and Pitzer [20]. The apparent mass density of dissolved CO_2 is predicted with Eq. (13) proposed in this work. As shown in Fig. 7, an intersection is obtained at a certain temperature, which can be named as equal density temperature (T_e) proposed by Lu et al. [17]. The results in Fig. 7 revealed that the T_e of Dagang - formation at 20 MPa (466.5 K) is slightly higher than that of 10 MPa (464.67 K). The salinity of Dagang brine is very small and the brine belongs to brackish water. Thus, the result is close to the T_e of pure water in Hnedkovsky et al. [22], which is 473.35 K as shown in Fig. 8. Meanwhile, the T_e of pure water at 35 MPa can also be obtained as 483.26 K from Fig. 8. Therefore, the equal density temperature increases with increasing pressure, although the increment is not so obvious. As shown in Fig. 7, the T_e are 466.5 K and 459.57 K for the brine salinity 0.08027 and 1 mol/kg NaCl at 20 MPa, respectively. It means that T_e decreases with increasing salinity of brine, which is consistent with the results reported in Lu et al. [18].

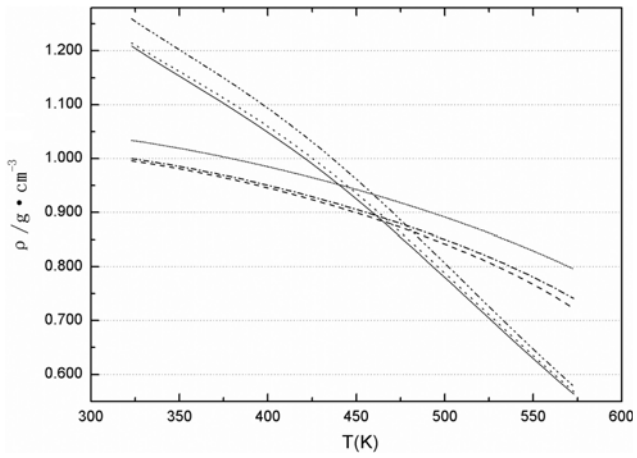

Fig. 7. Density of CO_2-free brine (Dagang - formation: dash line, 10 MPa; dash dot line, 20 MPa. 1 mol/kg NaCl: short dot line, 20 MPa) and apparent mass density of dissolved CO_2 (Dagang - formation: solid line, 10 MPa; dot line, 20 MPa. 1 mol/kg NaCl: dash dot dot line, 20 MPa) as a function of temperature.

It is generally believed that the densities of water/brine dissolved with CO_2 are higher than that of CO_2 - free water/brine in common temperature and pressure conditions in previous researches [14,21]. However, when the temperature is higher than the equal density temperature, the density of water/brine with CO_2 dissolved will be lower than that of CO_2 - free water/brine. A possible explanation is that the density decrease caused by the rise of temperature is larger than the density increase due to the dissolution of CO_2 for brine under high temperature conditions. So the solution density decreases after CO_2 dissolved and the solution will migrate upward due to buoyancy, which would increase the risk of CO_2 leakage. This is not conducive to CO_2 geologic sequestration. Therefore, the saline aquifers with high geothermal gradient are not suitable for CO_2 sequestration. In this work the formation temperature of the Dagang oilfield reservoir is from 313.15 K to 363.15 K, which is lower that the equal density temperature 464.67 K. Therefore, the safety of CO_2 storage can be guaranteed.

CONCLUSIONS

Densities of CO_2+Dagang - formation brine were measured in

the pressure range from (10 to 18) MPa, temperatures from (313.15 to 363.15) K and CO_2 mass fractions up to 0.0299 by a MSB. It was found that (1) For a given CO_2 concentration, the densities of CO_2+Dagang - formation brine were approximately linearly proportional to pressure, and the slopes at different concentrations were almost the same at a constant temperature. (2) The dissolution of CO_2 in brine would increase the solution density in common conditions. For the same temperature and pressure conditions, the densities of CO_2+Dagang - formation brine increased with increasing CO_2 mass fraction almost linearly in our experimental range. But the slopes of the experimental densities *vs.* CO_2 mass fractions decreased from (0.193 to 0.106) g·cm^{-3} with the temperature increased from (313.15 to 363.15) K. (3) A correlation equation was developed based on thermodynamic theory and experimental data. For the density of CO_2+water/brine solution in geological sequestration conditions, the absolute average deviation between the model and the experimental data was 0.05% and the maximum deviation was 0.37%. (4) The equal density temperature of Dagang - formation is 464.67 K and 466.5 K at 10 MPa and 20 MPa, respectively. The formation temperature of the Dagang oilfield reservoir is from 313.15 K to 363.15 K, which is lower that the equal density temperature. Therefore, the safety of CO_2 storage can be guaranteed. While, the saline aquifers with high salinity and high temperature are not the best sites for the CO_2 geological sequestration.

ACKNOWLEDGEMENT

The authors thank the editor and the reviewers for their valuable comments. This work has been supported by Liaoning Provincial Natural Science Foundation of China (201202028), National Natural Science Foundation of China (No. 51006016 & 51106019), National Program on Key Basic Research Project (No. 2011CB707304) and the Fundamental Research Funds for the Central Universities.

Notes

The authors declare no competing financial interest.

NOMENCLATURE

T : temperature
P : pressure
ρ(T, P) : density of measured solution under (T, P) condition
m_0 : mass of sinker in vacuum
m′(T, P) : apparent mass of sinker under (T, P) condition
v(T, P) : volume of sinker under measuring condition (T, P)
U(ρ) : uncertainty of the solution density
$U_d(\rho)$: uncertainty caused by measured density
U(w) : uncertainty caused by CO_2 mass fraction
U_{m_0}, $U_{m'}$, U_v : uncertainty caused by m_0, m′, v
T_0, P_0 : reference state
α_T : isobaric thermal expansion coefficient
K_T : isothermal compressibility module
L_0 : original length of the sinker
ΔL : length change of the sinker
E : Young's modulus
γ : Poisson's ratio
V_m : molar volume of the CO_2+brine solution
x_1, x_2 : the mole fractions of brine and CO_2
V_1 : molar volume of brine
V_2^{ϕ} : apparent molar volume of CO_2 dissolved in brine
M_1, M_2 : molecular weight of brine and CO_2
w_2 : mass fraction of CO_2
ρ^m : density of CO_2+brine solution
ρ_1^m : density of brine
$\rho_2^{m,\phi}$: apparent mass density of CO_2

REFERENCES

1. IPCC Third Assessment Report: Climate Change 2001 (TAR).
2. P. Englezos and J. D. Lee, *Korean J. Chem. Eng.*, **22**, 671 (2005).
3. J. D. Figueroa, T. Fout, S. Plasynski, H. McIlvried and R. D. Srivastava, *Int. J. Greenh. Gas Control.*, **2**, 9 (2008).
4. S. M. Benson and D. R. Cole, *Element*., **4**, 325 (2008).
5. A. Anissa, H. R. Muhammad, L. Faical AND A. Abbaci, *Korean J. Chem. Eng.*, **31**(6), 1043 (2014).
6. U. Zahid, Y. Lim, J. Jung and C. Han, *Korean J. Chem. Eng.*, **28**(3), 674 (2011).
7. X. Ji, S. P. Tan, H. Adidharma and M. Radosz, *Ind. Eng. Chem. Res.*, **44** (22), 8419 (2005).
8. I. S. Khattab, F. Bandarkar, M. A. Fakhree and A. Jouyban, *Korean J. Chem. Eng.*, **29**(6), 812 (2012).
9. P. M. Haugan and H. Drange, *Nature*, **357**, 318 (1992).
10. H. Drange and P. M. Haugan, *Energy Convers. Manage.*, **33**(5-8), 697 (1992).
11. T. Ohsumi, N. Nakashiki, K. Shitashima and K. Hirama, *Energy Convers. Manage.*, **33**(5-8), 685 (1992).
12. Y. Song, B. Chen, M. Nishio and M. Akai, *Energy*, **30**(11-12), 2298 (2005).
13. Z. Li, M. Dong, S. Li and L. Dai, *J. Chem. Eng. Data*, **49**(4), 1026 (2004).
14. Y. Zhang, F. Chang, Y. Song, J. Zhao, Y. Zhan and W. Jian, *J. Chem. Eng. Data*, **56**(3), 565 (2011).
15. Y. Song, W. Jian, Y. Zhang, M. Yang, J. Zhao, Y. Liu, W. Liu and Y. Shen, *J. Chem. Eng. Data*, **59**, 1400 (2011).
16. W. Yan, S. Huang and E. H. Stenby, *Int. J. Greenh. Gas. Control*, **5**(6), 1460 (2011).
17. J. Hu, Z. Duan, C. Zhu and I. Chou, *Chem. Geol.*, **238**(3-4), 249 (2007).
18. C. Lu, W. S. Han, S. Y. Lee, B. J. McPherson and P. C. Lichtner, *Adv. Water Res.*, **32**(12), 1685 (2009).
19. P. Karsten and S. Nicolas. *Energy Convers. Manage.*, **48**, 1761 (2007).
20. P. S. Z. Rogers and K. S. Pitzer, *J. Phys. Chem. Ref. Data*, **11**(1), 15 (1982).
21. J. E. Garcia, *Lawrence Berkley National Laboratory Report*, LBNL 49023 (2001).
22. L. Hnedkovsky, R. H. Wood and V. Majer. *J. Chem. Thermodyn.*, **28**(2), 125 (1996).
23. Y. Song, M. Nishio, B. Chen, S. Someya and T. Ohsumi, *J. Visualization.*, **6**, 41 (2003).
24. M. B. King, A. Mubarak, J. D. Kim and T. R. Bott, *J. Supercrit. Fluids*, **5**(4), 296 (1992).
25. A. Hebach, A. Oberhof and N. Dahmen, *J. Chem. Eng. Data*, **49**(4), 950 (2004).